



Observations of Electron Fluxes in the Radiation Belts with PROBA-V/EPT at Polar Low Earth Orbit and Van Allen Probes/MagEIS at Near Equatorial Elliptical Orbit

Viviane Pierrard*^(1,2), Edith Botek⁽¹⁾, Jean-François Ripoll^(3,4), G. Reeves⁽⁵⁾ and S. A. Thaller⁽⁶⁾

- (1) Royal Belgian Institute for Space Aeronomy, Brussels, B-1180, Belgium, <http://www.aeronomie.be>
(2) Center for Space Radiations, ELI-C, Université Catholique de Louvain, Louvain-La-Neuve, Belgium
(3) CEA, DAM, DIF, F-91297 Arpajon, France
(4) UPS, CEA, LMCE, 91680 Bruyères-le-Châtel, France
(5) Los Alamos National Laboratory, NM, United States
(6) Laboratory for Atmospheric and Space Physics, University of Colorado, Boulder, CO, United States

Abstract

The electron fluxes in the outer radiation belt during and after geomagnetic storms were investigated using the EPT (Energetic Particle Telescope) instrument on board the ESA PROBA-V satellite at a polar LEO (Low Earth Orbit) at 820 km of altitude and compared with simultaneous observations of the instrument MagEIS on board the NASA Van Allen Probes circulating on a low inclination elliptical orbit ranging from 600 to 30 600 km.

We find that the equatorial trapped electron fluxes observed at MEO (Medium Earth Orbit) are higher than at LEO. Below 1 MeV, maximal fluxes differ by ~2 orders of magnitude. However, the EPT ultra-relativistic flux (>2.4 MeV) is much lower than the Van Allen Probes flux at 2.33 MeV, by 4 to 5 orders of magnitude. We also observe that the outer belt is quite isotropic during quiet times, contrary to the inner belt. During storms (here, the big storm of 23 June 2015), the dropout and flux increase observed at LEO and MEO present very similar shapes.

1. Introduction

The ESA satellite PROBA-V had provided flux observations from EPT on a LEO polar orbit at an altitude of 820 km since its launch in May 2013. The inclination is 98.73°, the orbital rotation period has a duration of 101.21 minutes and 10:30 AM is the nominal local time at the descending node. The EPT detector measures the electron fluxes above 500 keV, in addition to protons above 9.5 MeV [1].

The NASA Van Allen Probes mission, formerly called RBSP (Radiation Belt Storm Probes A and B) was launched in 2012 [2]. It operated simultaneously with EPT from 2013 to 2019, enabling unprecedented studies of the electron radiation belt variability in response to solar activity. RBSP flew on a low inclination (<20°) elliptical orbit ranging from 600 to 30,600 km. The MagEIS

(Magnetic Electron Ion Spectrometer) instrument observed electrons in the energy range from 30 keV to 4 MeV.

The comparison of electron fluxes measured by EPT at LEO with those of MagEIS close to the equatorial plane, combined with simulations, helps us to understand the dynamics of the radiation belts [3].

2. Analysis of the Observations

Figure 1 shows the EPT electron fluxes from 18 June 2015 up to 28 June 2015 (horizontal axis), as a function of the McIlwain parameter L (vertical axis) for the 6 electron energy channels. A very big storm is observed on 23 June 2015 with a Disturbed Storm Time index $Dst = -204$ nT. A dropout is clearly visible for all energy channels of EPT (> 500 keV), as is observed for all Dst events [3]. The dropout has a V-shape, i.e., starts earlier and has a longer duration at high L than at lower L , following the Dst shape well [4]. The dropout is followed by a strong flux enhancement in the outer belt and in the slot region to a lower L value than before the storm. Contrary to the dropout, such penetration in the slot is only observed for the strongest storms, and the depth is proportional to the Dst intensity [4]. It can even reach the inner belt, but not for $E > 2.4$ MeV in EPT observations [5]. After the storm, the flux gradually decays with time, especially in the slot region that reappears a few days after the storms [6]. There is almost no electron flux with $E > 2.4$ MeV in the inner belt, probably due to low radial diffusion creating a barrier [7] limiting the penetration of these electrons at low distances [4].

The NASA Van Allen Probes have four magnetic spectrometers aboard each of the two spacecraft, one low-energy unit (20–240 keV), two medium-energy units (80–1200 keV), and a high-energy unit (800–4800 keV), allowing us to analyze also what happens for lower energies. Figure 2 shows RBSP B observations using the ETC combined flux [8] for the same period from 18 to 28 June 2015. At sub-relativistic and relativistic energy (last 4 panels), the radiation belt is concentrated in the outer belt

above $L \sim 4$ before the storm of 23 June and a slot is clearly visible (above $L \sim 2.3$ for $E=465$ keV for instance), contrary to what is observed at lower energies (4 first panels) where the more intense fluxes are concentrated at $L < 4$, with an outer edge increasing in L when E decreases. The 1 MeV fluxes and above are closer to the inner belt than sub-relativistic electron fluxes during the quiet period. This is due to the fact that sub-relativistic electrons ($\sim < 1$ MeV) are more sensitive to whistler-mode hiss waves than higher energy electrons, with these interactions occurring at higher L -shell for the sub-relativistic electrons, and thus are more scattered during extended quiet periods [9, 10, 11].

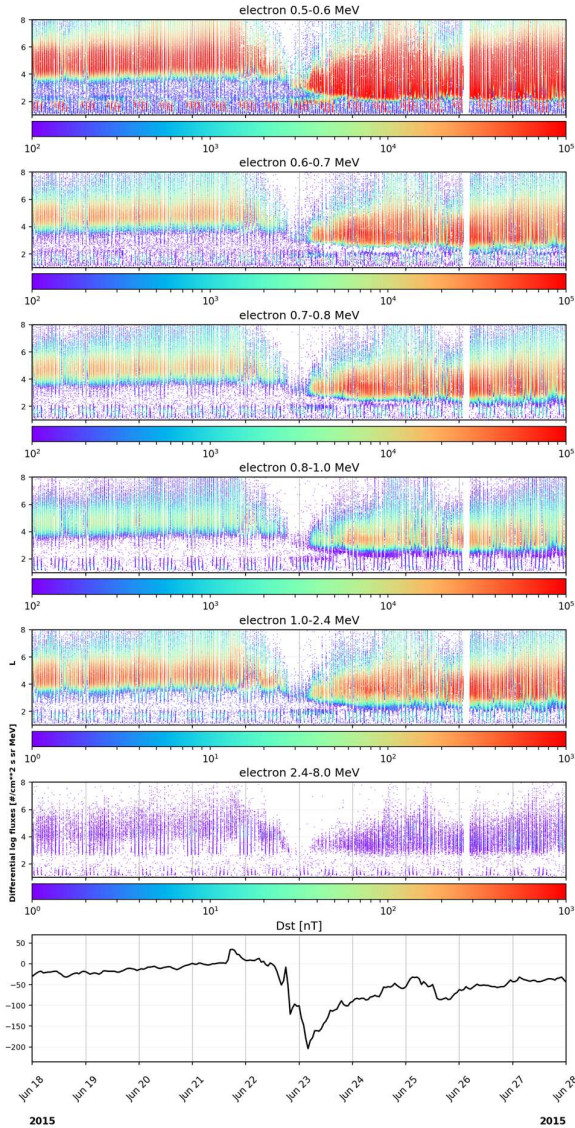


Figure 1. Electron fluxes observed by EPT from 18 June 2015 up to 28 June 2015, as a function of the McIlwain parameter L (vertical axis) and time (horizontal axis) for the 6 electron energy channels. The observed Dst (Disturbed Storm Time) index is given in the bottom panel.

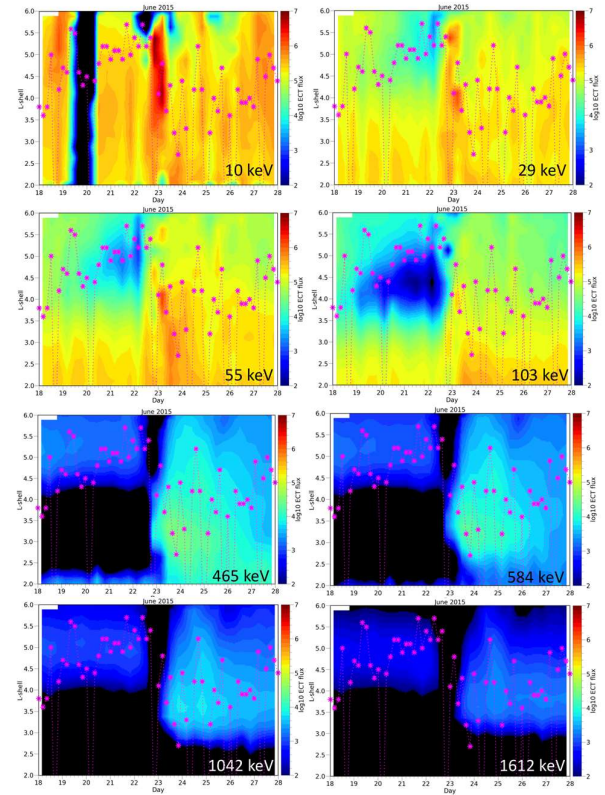


Figure 2. Electron fluxes (in $\#/(cm^2 s sr keV)$) versus time and L -shell measured by RBSP instruments from 18 June 2015 up to 28 June 2015 (for the storm period of 23 June 2015 as in Figure 1). The 4 first panels show low energy seed electrons (10 to 103 keV), which contribute to the electromagnetic environment and as source of aurora. The 4 next panels show radiation belt flux for sub-relativistic and relativistic electrons (from 465 keV to 1.612 MeV). The magenta dotted line corresponds to the plasmapause position measured by spacecraft charging using EFW on RBSP B.

In Figure 2, the dropout has also some trace of a V-shape and seems to penetrate at lower L when the energy is high ($L \sim 4.5$ at 465 keV while $L \sim 4$ at $L > 1$ MeV). This is also observed with EPT at LEO, but with a lower penetration ($L \sim 3.9$ at 500 keV, $L \sim 3$ at $E > 2.4$ MeV). At energies $E < 103$ keV, the dropout is almost not visible, which is a rare feature as dropout by definition should remove all particles. This may indicate fast substorm injections occur in a close timeframe. The temporal binning generated in Figure 2 may also be too coarse to analyze the details of these fast processes. During the storm, the flux penetration at lower L is also clearly observed, with an injection reaching the inner belt up to $E=584$ keV like in EPT measurements.

3. Discussion

Other comparisons have been made recently to study the causes of flux variations. The comparison of magnetopause position and of the dropout depth have indicated that

dropouts are the consequence of magnetopause shadowing, i.e., the removal of the outer radiation belt electrons from the inner magnetosphere when a higher flux of solar wind pushes the magnetopause closer to the Earth [12]. Simulations of the particle motion also show that the dropout is also due to the outward drift motion of the particles associated to the perturbation of the magnetic field [12].

The gradual flux decay observed in the slot and the outer belt in the 0.1-1 MeV range seems more related to wave-particle interactions, especially with plasmaspheric hiss [9, 10, 11]. Due to the strong electron interactions between the energetic particles trapped in the radiation belts and plasmaspheric hiss, the exact position of the plasmopause boundary, as well as the density of the low energy background particles inside and outside the plasmasphere is critical to know. The EFW instrument on board Van Allen Probes allowed the deduction of the plasmopause position, as shown in Figure 2 by the magenta line. When no observations are available, the SWIFF plasmasphere model can be used to determine the position of the plasmopause and the density inside and outside the plasmasphere [13]. The model has been recently improved for the plasmatrough part by using Van Allen Probes observations outside the plasmasphere [14].

Other waves can also cause the loss of electrons, including those with anthropogenic origins: the very low-frequency transmitter in the Northwest Cape of Australia (NWC) has recently been observed to pitch-angle scatter electrons up to 800 keV, using EPT measurements [15]. The radiation belt particles also interact with the other regions of the magnetosphere as attested by the observed links between the plasmopause, the ionospheric convection, the boundaries of the radiation belts, and the auroral oval [11].

4. Acknowledgements

The authors thank the CSR team for the EPT data validation and the EFW, EMFISIS and MagEIS teams of the Van Allen Probes mission for their support. International Space Sciences Institute (ISSI) and the participants in a 2020 ISSI workshop for the project “Radiation belts physics”. This work has received funding from the European Union’s Horizon 2020 research and innovation programme under grant agreement No 870437 for the SafeSpace (Radiation Belt Environmental Indicators for the Safety of Space Assets) project, and for the PITHIA-NRF project (funding from the European Union’s Horizon 2020 research and innovation programme under grant agreement No 101007599).

References

[1] V. Pierrard, G. Lopez Rosson, K. Borremans, J. Lemaire, J. Maes, Bonnewijn, S., et al., The Energetic Particle Telescope: First results, *Space Science Rev.*, **184**, 1, 2014, pp. 87-106, doi: 10.1007/s11214-014-0097-8.

[2] B. H. Mauk, N. J. Fox, Kanekal S. G., Kessel R. L., Sibeck D.G., and A. Ukhorskiy, Science objectives and rationale for the Radiation Belt Storm Probes mission, *Space Science Review*, **179**, 2013, pp. 1-4, doi: 10.1007/s11214-012-9908-y.

[3] J.-F. Ripoll, Claudepierre S. G., Ukhorskiy A. Y., Colpitts C., Li X., Fennell J., & Crabtree C., Particle Dynamics in the Earth’s Radiation Belts: Review of Current Research and Open Questions. *Journal of Geophysical Research: Space Physics*, **125**, 2020, e2019JA026735, doi: 10.1029/2019JA026735

[4] V. Pierrard, Botek E., Ripoll J.-F., and G. S. Cunningham, Electron dropout events and flux enhancements associated with geomagnetic storms observed by PROBA-V/EPT from 2013 to 2019, *Journal of Geophysical Research: Space Physics*, **125**, 12, 2020, e2020JA028487, doi: 10.1029/2020JA028487

[5] V. Pierrard, G. Lopez Rosson, E. Botek, Dynamics of Mega-electron Volt Electrons Observed in the Inner Belt by PROBA-V/EPT, *Journal of Geophysical Research: Space Physics*, **124**, 2019, pp. 1651-1659, doi: 10.1029/2018JA026289.

[6] V. Pierrard, G. Lopez Rosson, The effects of the big storm events in the first half of 2015 on the radiation belts observed by EPT/PROBA-V, *Annales Geophysicae*, **34**, 2016, pp. 75-84, doi: 10.5194/angeo-34-75-2016.

[7] D. N. Baker, Jaynes A. N., Hoxie V. C., Thorne R. M., Foster J. C., Li X., et al., An impenetrable barrier to ultrarelativistic electrons in the Van Allen radiation belts. *Nature*, **515**(7528), 2014, pp. 531–534, doi: 10.1038/nature13956

[8] A. J. Boyd, Reeves, G. D., Spence, H. E., Funsten, H. O., Larsen, B. A., Skoug, R. M., et al., RBSP-ECT combined spin-averaged electron flux data product. *Journal of Geophysical Research: Space Physics*, **124**, 2019, pp. 9124 - 9136, doi: 10.1029/2019JA026733

[9] J.-F. Ripoll, Loridan V., Denton M. H., Cunningham G., Reeves G., Santolík O., et al., Observations and Fokker-Planck simulations of the L-shell, energy, and pitch angle structure of Earth’s electron radiation belts during quiet times, *Journal of Geophysical Research: Space Physics*, **124**, 2019, doi: 10.1029/2018JA026111

[10] J.-F. Ripoll, Loridan V., Denton M. H., Cunningham G., Reeves G., Santolík O., et al., Observations and Fokker-Planck simulations of the L-shell, energy, and pitch angle structure of Earth’s electron radiation belts during quiet times, *Journal of Geophysical*

Research: Space Physics, **124**, 2019, doi:
10.1029/2018JA026111

- [11] V. Pierrard, E. Botek, J.-F. Ripoll, S. A. Thaller, M. B. Moldwin, M. Ruohoniemi, and G. Reeves, Links of the plasmopause with other boundary layers of the magnetosphere: ionospheric convection, radiation belts boundaries, auroral oval, *Frontiers in Astronomy and Space Sciences*, Coupled Feedback Mechanisms in the Magnetosphere-Ionosphere System, November 2021, doi: 10.3389/fspas.2021.728531.
- [12] V. Pierrard, J.-F. Ripoll, G. Cunningham, E. Botek, O. Santolik, S. Thaller, W. Kurth, and M. Cosmides, Observations and simulations of dropout events and flux enhancements in October 2013: Comparing MEO equatorial with LEO polar orbit, *Journal of Geophysical Research: Space Physics*, **126**, May 2021, e2020JA028850, doi: 10.1029/2020JA028850.
- [13] V. Pierrard, E. Botek, and F. Darrouzet, Improving Predictions of the 3D Dynamic Model of the Plasmasphere, *Front. In Astron. Space Sci.*, 8:681401, pp. 1-8, May 2021, doi: 10.3389/fspas.2021.681401
- [14] E. Botek, V. Pierrard, and F. Darrouzet, Assessment of the Earth's cold plasmatrough modeling by using Van Allen Probes/EMFISIS and Arase/PWE electron density data, *Journal of Geophysical Research: Space Physics*, **126**, 12, December 2021, doi: 10.1029/2021JA029737.
- [15] G. S. Cunningham, E. Botek, V. Pierrard, C. Cully and J.-F. Ripoll, Observation of High-Energy Electrons Precipitated by NWC Transmitter from PROBA-V Low-Earth Orbit Satellite, *Geophysical Research Letters*, **47**, 16, July 2020, e2020GL089077, doi: 10.1029/2020GL089077.